SURFACE SCIENCE LABORATORIES

ANALYSIS REPORT

University of Alabama in Huntsville

Huntsville, AL 35899

(NASA-CR-183572) AUGER AND ESCA ANALYSIS Final Report (Alabama Univ.) 22 p CSCL 07D

N89-24463

Unclas
G3/25 0192824

Final Report on NASA Contract NAS8-36955

Delivery Order #9 - Report #727

entitled

Auger and ESCA Analysis

Prepared by

J C Gregory

John C. Gregory, Principal Investigator
The University of Alabama in Huntsville

Department of Chemistry
College of Science
Huntsville, AL 35899
(205) 895-6028

ANALYSIS REPORT

CUSTOMER NAME: Ilmars Dalins

CUSTOMER ADDRESS: NASA Marshall Space Flight Center
Huntsville, AL
Phone: (205) 544-2573

ANALYSIS DATES: September 14,15,16,17,18,19,20,21, 1988

INVESTIGATOR: Dr. M.J. Edgell

UAH SURFACE SCIENCE LABORATORIES

The Surface Science Laboratories at the University of Alabama in Huntsville (UAH) are equipped with x-ray photoelectron spectroscopy (XPS or ESCA) and Auger electron spectroscopy (AES) facilities. These techniques provide information from the uppermost atomic layers of a sample, and are thus truly surface sensitive.

The XPS instrument is a Perkin-Elmer 5400 system. XPS provides both elemental and chemical state information without restriction on the type of material that can be analyzed. The sample (up to 0.75 inch in size) is placed into an ultra high vacuum (UHV) chamber and irradiated with x-rays which cause the ejection of photoelectrons from the sample surface. MgKα and AlKα are the standard sources available on the 5400 system, but a Zr Lα anode may also be used on the UAH instrument. Since the kinetic energy of these emitted electrons is characteristic of the elements from which they were ejected, the position and intensity of the peaks in an energy spectrum provide the desired analytical information. The chemical state of an atom alters the binding energy of a photoelectron and thus its emitted kinetic energy. Thus, bonding information is derivable from these chemical shifts and also from the shapes of the peaks. Since x-rays do not normally cause charging problems or beam damage, XPS is

applicable to a wide range of samples including metals, polymers, catalysts and fibers. Samples can be analyzed to as small an area as 200 μm using the "small area" XPS system.

The AES instrument is a Kratos Analytical XSAM 800 system. AES uses a beam of high energy electrons as a surface probe. Following electronic rearrangements within excited atoms by this probe, Auger electrons characteristic of each element present are emitted from the sample. As in the case of the x-ray photoelectrons, only those Auger electrons which emerge from the topmost atomic layers contribute to the spectrum, hence the high surface specificity of this technique. AES detects all elements other than hydrogen and helium usually to a sensitivity better than 1 atom percent of a monolayer. The electron gun on the UAH XSAM can be focused to produce a beam of diameter 1000Å, allowing high spatial resolution analyses, otherwise known as scanning Auger microscopy (SAM), to be performed. On the rastering of this beam synchronously with a video display using established scanning electron microscopy techniques, physical images and chemical distribution maps of the surface can be produced. Thus very small features, such as electronic circuit elements or corrosion pits in metals, can be investigated.

Facilities are available on both XPS and AES instruments for depth-profiling of materials, using a beam of argon ions to sputter away consecutive layers of material to reveal sub-surface

(and even semi-bulk) analyses. Generally, AES is the preferable technique for such work, since its spatial resolution capacity is much better.

For further information on facilities available at the UAH Surface Science Laboratories contact Dr. J.C. Gregory at 895-6028 or Dr. M.J. Edgell at 895-6076.

CUSTOMER NAME: Ilmars Dalins

DATE: September 14,15,16,17,18,19,20,21, 1988

INVESTIGATOR: Dr. M.J. Edgell

ANALYSIS OF FRACTURED STRUT SAMPLE

A sample was provided for XPS and AES analysis by Ilmars Dalins of the NASA Marshall Space Flight Center in Huntsville, Alabama.

The sample consisted of a small, recently exposed fractured surface (shiny) and a larger fractured surface that had been exposed to high temperatures (darkened).

It was thought that the shiny surface should have a relatively thin oxide layer at its surface, while the oxide on the darkened surface was thought to be ≥ 1 μm thick. The darkening was thought due to Cr_2O_3 layer presence at the surface.

Analysis was performed at UAH to determine surface species present, and oxide primary constituents, using both XPS and AES. Various areas on the sample were identified for analysis, these being shown as A-E in Figure 1.

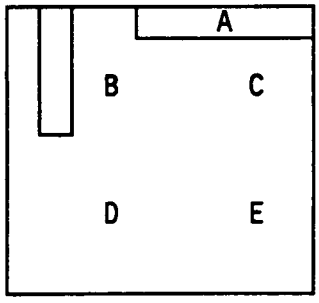

Figure 1

TECHNIQUES USED: XPS

Mg Kα radiation (hν = 1253.6) was used throughout for XPS analysis.

Unless specifically noted within the text, survey scans are required using an analyzer pass energy of 89.45 eV, while multiplex scans are required using an analyzer pass energy of 35.75 eV. Analysis is generally conducted in the "large aperture" mode, i.e. the energy analyzer is accepting electrons from an area of 1.1 mm^2, while samples are analyzed at an angle of 45°.

Typical spectrometer operating specifications include:

Pressure: 10^{-9} Torr

X-ray anode power: 300 watts

Ion gun conditions: 4 KV, 79% focus, 25mA

TECHNIQUES USED: AES

A 10 KV electron beam was used throughout for AES analysis.

Unless specifically noted within this text, spectra are acquired with the energy analyzer in the higher magnification mode, with a retard ratio of 10.60 (analyzer mode FRR).

Where possible, analyses are acquired in the highest resolution (1000 Å) mode.

XPS RESULTS

1) Fresh fracture (Area A)

The survey spectrum for this area can be seen in Figure X2. Principal elements recorded are carbon (284 eV), oxygen (532 eV) and silicon (100 and 150 eV) - elements such as iron, chromium and nickel are less strongly present, since they are below the level of surface being analyzed.

Figure X3 - X22 display the higher resolution multiplex scans for elements C, O, Si, N, Na, Cl, P, S, Cr, Ni, Mo, Nb, Ta, Ti, Al Co, B, Cu, Fe, and Mn.

From these spectra, relative atomic concentrations were calculated and are shown in Table 1.

2) Temperature-exposed fracture (Area B)

The survey spectrum for this area can be seen in Figure X23. Principal elements recorded are carbon, oxygen, silicon, and nickel (840 eV). Figures X24-X43 display the higher resolution multiplex scans for the elements as listed previously (1). Notable differences from Area A included the strong presence of nickel, together with smaller concentrations of Nb and Cu and trace presence of Cr, Mo, Al and Cu.

From these spectra, relative atomic concentrations were calculated and are shown in Table 2.

Table 1 Atomic Concentrations (Area A)

Element	Sensitivity Factor	Concentration (%)
C 1s	0.296	66.0
O 1s	0.711	27.6
N 1s	0.473	-
Si 2p	0.339	6.4
Na 1s	1.685	-
Cl 2p	0.891	-
P 2p	0.486	-
S 2p	0.666	-
Cr 2p	2.427	-
Ni 2p	4.044	-
Mo 3d	3.321	-
Nb 3d	2.921	-
Ta 4f	3.082	-
Ti 2p	2.001	-
Al 2p	0.234	-
Mn 2p	2.659	-
Co 2p	3.590	-
B 1s	0.159	-
Cu 2p	5.321	-
Fe 2p	2.957	tr

tr = trace

Table 2 Atomic Concentrations (Area B)

Element	Sensitivity Factor	Concentration (%)
C 1s	0.296	47.9
O 1s	0.711	37.3
N 1s	0.473	-
Si 2p	0.339	8.7
Na 1s	1.685	-
Cl 2p	0.891	tr
P 2p	0.486	-
S 2p	0.666	-
Cr 2p	2.427	tr
Ni 2p	4.044	5.4
Mo 3d	3.321	tr
Nb 3d	2.921	0.2
Ta 4f	3.082	-
Ti 2p	2.001	-
Al 2p	0.234	tr
Mn 2p	2.659	-
Co 2p	3.590	tr
B 1s	0.159	-
Cu 2p	5.321	0.4
Fe 2p	2.957	tr
(Pb)		

tr = trace

Table 3 Atomic Concentrations (Area C)

Element	Sensitivity Factor	Concentration (%)
C 1s	0.296	52.0
O 1s	0.711	33.2
N 1s	0.473	-
Si 2p	0.339	8.7
Na 1s	1.685	-
Cl 2p	0.891	-
P 2p	0.486	-
S 2p	0.666	-
Cr 2p	2.427	2.0
Ni 2p	4.044	3.1
Mo 3d	3.321	-
Nb 3d	2.921	0.7
Ta 4f	3.082	-
Ti 2p	2.001	tr
Al 2p	0.234	tr
Mn 2p	2.659	tr
Co 2p	3.590	tr
B 1s	0.159	-
Cu 2p	5.321	0.3
Fe 2p	2.957	tr
(Pb)		

tr = trace

Table 4 Atomic Concentrations (Area D)

Element	Sensitivity Factor	Concentration (%)
C 1s	0.296	60.1
O 1s	0.711	30.4
N 1s	0.479	-
Si 2p	0.339	6.1
Na 1s	1.685	-
Cl 2p	0.891	-
P 2p	0.486	-
S 2p	0.666	tr
Cr 2p	2.427	tr
Ni 2p	4.044	2.8
Mo 3d	3.321	-
Nb 3d	2.921	-
Ta 4f	3.082	-
Ti 2p	2.001	tr
Al 2p	0.234	tr
Mn 2p	2.659	tr
Co 2p	3.590	-
B 1s	0.159	-
Cu 2p	5.321	0.5
Fe 2p	2.957	tr
(Pb)		

tr = trace

3) Temperature-exposed fracture (Area C)

The survey spectra for this area can be seen in Figure X44. Principal elements recorded are carbon, oxygen, silicon, nickel, chromium and possibly copper.

Figures X45-X64 display the higher resolution multiplex scans for the elements as listed previously (1). Notable differeneces from Area A include the strong presence of Ni, Cr, Nb and Cu and trace concentrations of Ti, Al Mn and Co.

From these spectra, relative atomic concentrations were calculated and are shown in Table 3.

4) Temperature-exposed fracture (Area D)

The survey spectra for this area can be seen in Figure X65. Principal elements recorded are carbon, oxygen, silicon, nickel and copper.

Figure X66-X85 display the higher resolution multiplex scans for the elements as listed previously (1). Notable differences from Area A include the strong presence of Ni and Cu, and trace concentrations of S, Cr, Ti, Al and Mn.

From these spectra, relative atomic concentrations were calculated and are shown in Table 4.

5) Temperature-exposed fracture (Area E)

The survey spectra for this area can be seen in Figure X86. Principal elements recorded are carbon, oxygen, silicon, nickel, chromium and copper.

Figures X87-X106 display the higher resolution multiplex scans for the elements as listed previously (1). Notable differences from Area

A include the strong presence of Ni, Cr, and Cu, and trace concentrations of niobium.

From these spectra, relative atomic concentrations were calculated and are shown in Table 5.

N.B. Figure X107 shows a multiplex scan for the Pb 4f line. This appears in the same area as phosphorous (2p), but is present as a widely spaced doublet. There appears to be ($\leq$ 0.4%) lead presence is a contaminant in all areas except A. Thus this could have occurred as a result of the heating process. (unlike the silicon contamination which is present on all areas, probably originating from the cutting process).

For ease of comparison, atomic percentages from the different areas have been listed together in Table 6.

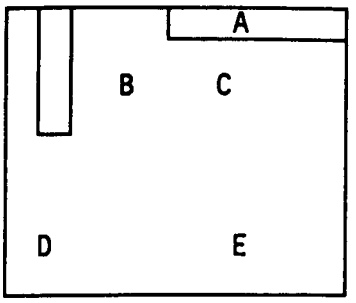

Table 6: Summary of XPS Results

%	Area A	Area B	Area C	Area D	Area E
C	66.0	47.9	52.0	60.1	57.8
O	27.6	37.3	33.2	30.4	31.4
N	-	-	-	-	-
Si	6.4	8.7	8.7	6.1	4.1
Na	-	-	-	-	-
Cl	-	tr	-	-	-
P	-	-	-	-	-
S	-	-	-	tr	-
Cr	-	tr	2.0	tr	1.7
Ni	-	5.4	3.1	2.8	4.2
Mo	-	tr	-	-	-
Nb	-	0.2	0.7	-	tr
Ta	-	-	-	-	-
Ti	-	-	tr	tr	-
Al	-	tr	tr	tr	-
Mn	-	-	tr	tr	-
Co	-	tr	tr	-	-
B	-	-	-	-	-
Cu	-	0.4	0.3	0.5	0.8
Fe	tr	tr	tr	tr	tr
(Pb)					

AES RESULTS

Due to the increased resolution available using AES, this technique was primarily used for elemental mapping and profiling to determine relative distributions present in the sample. Unfortunately the high degree of surface roughness on the fracture sample caused a severe decrease in signal intensity available particularly for surface analysis (as was the case with XPS), causing acquisition time to be lengthened. Furthermore, since ideal sputter profiling should involve the profiling ion beam and the analyzing electron beam to be at the same point on the sample, surface roughness can again interfere.

A similar approach was adopted as that for XPS, with five areas identified of interest. (Since XPS and AES analysis was performed in separate instrumentation, identical areas could not be selected).

1) Fresh fracture (Area A)

This area appeared considerably less rough than other areas on the sample. The micrograph in Figure A1 is of magnification x100.

The survey spectra for this region is shown in Figure A2, with carbon (270), oxygen (505) and silicon (1615) showing strongly. Higher resolution scans are shown in Figures A3 (carbon), A4 (oxygen & chromium), A5 (oxygen differentiated), A6 (nickel & iron), A7 (nickel differentiated) and A8 (silicon).

This area was then profiled using a 3kV Ar^+ ion beam, set to large size and raster. This produced a relatively small surface etch rate.

The results of approximately 350Å material removed are shown in Figures A9 - A12. These are overlaid spectra for carbon, oxygen & chromium, nickel & iron and silicon. For ease of comparison, the spectra following sputtering for oxygen/chromium and nickel/iron are shown in N(E) form in Figures A13 and A14, and in differentiated form in Figures A15 and A16. The increase of relative amounts of chromium (525 and 489 eV), nickel (848, 775 and 716 eV) and iron (703 and 651 eV) can be seen.

The survey spectrum for this area following sputtering is shown in Figure A17 (differentiated form Figure A17A), which shows the increase in metallic species present.

The micrograph in Figure A1A is x200 magnification. This was used for elemental mapping. Maps for oxygen, chromium, nickel, and iron are shown in Figures A18 - A21.

2) Temperature-exposed fracture (Area B)

The rougher nature of this surface can be seen in Figures A22 and A23, micrographs of x100 and x200 magnification.

The survey spectra for this area can be seen in Figure A24. Higher resolution scans are also shown for carbon (A25), oxygen & chromium (A26), nickel & iron (A27), and silicon (A28).

Differentiated forms of oxygen & chromium and nickel & iron are shown in Figures A29 and A30.

3) Temperature-exposed fracture (Area C)

Electron micrographs of this area are shown in Figures A31 (x100) and A32 (x200).

The survey spectrum for this area can be seen in Figure A33. Higher resolution scans are also shown for carbon (A34), oxygen & chromium (A35), nickel & iron (A36) and silicon (A37). Differentiated forms of oxygen & chromium and nickel & iron are shown in Figures A38 and A39.

4) Temperature-exposed fracture (Area D)

Electron micrographs of this area are shown in Figures A40 (x100) and A41 (x200).

The survey spectrum for this area can be seen in Figure A42. Higher resolution scans are also shown for carbon (A43), oxygen & chromium (A44), nickel & iron (A45) and silicon (A46). Differentiated forms of oxygen & chromium and nickel & iron are shown in Figures A47 and A48.

5) Temperature-exposed fracture (Area E)

An electron micrograph of this area is shown in Figure A49 (magnification x200).

The survey spectrum for this area is shown in Figure A50, showing predominantly oxygen but some nickel. Higher resolution scans are shown for carbon (Figure A51), oxygen & chromium (A52), nickel & iron (A53) and silicon (A54). Differentiated forms for oxygen & chromium and nickel & iron are also shown in Figures A55 and A56.

This area was sputtered using similar beam conditions as those used in (1). Relative changes in spectra can be seen for carbon, oxygen & chromium, nickel & iron and silicon in Figures A57 - A60. For ease of comparison, the spectra following sputtering for oxygen/chromium and nickel/iron are shown in N(E) form in Figures A61 and A62, and in differentiated form in Figures A63 and A64. The increase in relative amounts of chroimium (525 and 489 eV), nickel 848, 775 and 716 eV) and iron (703 and 651 eV) can be seen.

The survey spectrum for this area following sputtering is shown in Figure A65, which shows the increase in metallic species (predominantly chromium) present.

Conclusions

Through XPS and AES analysis, it has been shown that the surface of the sample contains significant carbonaceous build-up together with silicon contamination (probably from the cutting of the sample) and possibly some lead contamination (origin unknown).

Clear differences exist physically and chemically between the "fresh" fracture and the heat-treated fracture, though variations

occur in the latter analysis position. Both forms of analysis show there to be very little iron at the surface; the oxide is (predominantly) a mixture of chromium and nickel oxides. Copper does appear fairly strongly in some analyses, as does niobium.

Chemical maps produced can be strongly affected by the surface roughness of a sample; therefore some features shown may be due to rapidly changing sample height, although topographical correction routines are designed to minimize such effects.